SnO_2 Extended Gate Field-Effect Transistor as pH Sensor

P. D. Batista[1], M. Mulato [1], C. F. de O. Graeff [1], F. J. R. Fernandez [2], and F. das C. Marques[3]
[1] *Departamento de Física e Matemática, FFCLRP-USP, Av. Bandeirantes, 3900, 14040-901, Ribeirão Preto, SP, Brazil*
[2] *PSI-Escola Politécnica-USP,*
[3] *DFA-IFGW-Unicamp*

Received on 4 April, 2005

Extended gate field-effect transistor (EGFET) is a device composed of a conventional ion-sensitive electrode and a MOSFET device, which can be applied to the measurement of ion content in a solution. This structure has a lot of advantages as compared to the Ion- Sensitive Field Effect Transistor (ISFET). In this work, we constructed an EGFET by connecting the sensing structure fabricated with SnO_2 to a commercial MOSFET (CD4007UB). From the numerical simulation of site binding model it is possible to determine some of the desirable characteristics of the films. We investigate and compare SnO_2 films prepared using both the Sol-gel and the Pechini methods. The aim is an amorphous material for the EGFET. The SnO_2 powder was obtained at different calcinating temperatures (200 - 500^{0}C) and they were investigated by X-ray diffraction (XRD), infrared spectroscopy (IR), thermogravimetric analysis (TGA) and differential thermal analysis (DTA). The films were investigated as pH sensors (range 2-11).

Keywords: SnO_2; pH sensor; Extended gate field-effect transistor

I. INTRODUCTION

Many chemical and biological processes depend on pH value, what makes it one of the commonest laboratory measurements. A recent development in pH measurement was the introduction of ion-sensitive field effect transistor (ISFET) technology as an alternative to the glass electrode [1,2]. The main part of an ISFET is the metal oxide silicon field effect transistor (MOSFET) with the gate electrode replaced by a chemically sensitive membrane. Recently, in the past four years, the extended gate field effect transistor (EGFET) was introduced as an alternative for the fabrication of ISFET [3]. EGFET is separated in two parts as shown in Fig. 1.

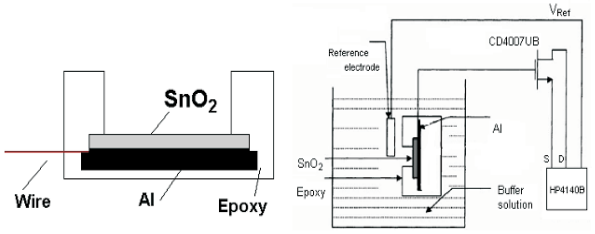

FIG. 1: Representation of EGFET structure and measurement system.

The sensitive part (at the left) is made of a SnO_2/Al structure and the system is completed with a commercial MOSFET CD4007UB (at the right).

This structure is easily constructed and has a lot of advantages when compared to the ISFET because it does not require the fabrication of the MOSFET.

The EGFET as pH sensor can be used to detect and to quantify any kind of substances that can produce or consume protons like an enzymatic reaction, therefore showing a large range of applications as biosensors [4].

In this work we implemented a numerical model to explain the interaction of the ion-sensitive membrane with charges in solution and discuss how some characteristics can affect the behavior of the sensor. Previous works have reported on the performance of sputtered [3] and sol-gel [5,6] fabricated SnO_2 EGFETs. The former is expensive and the latter did not work for the whole pH range. We investigate and compare cheaper alternative processes for the fabrication of SnO_2based EGFET: the sol-gel and Pechini methods. According to the present authors' knowledge, the Pechini's fabricated $SnO_2$was never used as ISFET of EGFET. The SnO_2powders were investigated by means of X-ray diffraction (XRD), infrared spectroscopy (FTIR), thermogravimetric analysis (TGA) and differential thermal analysis (DTA). The electrical response of the devices is also discussed.

II. SITE BINDING MODEL

The dependence of the surface potential on charge concentration can be explained with the well-known site-binding model theory. This was first introduced in 1974 by Yates *et. al* [7] to describe the properties of an oxide aqueous electrolyte interface and was generalized in 1986 by Fung *et. al.* [8] to characterize ISFETs with oxide gate insulators. According to the site-binding model, the oxide surface contains sites in three forms: SnO^-, SnOH, and $SnOH_2^+$. The surface potential (ψ) is dependent on the membrane material and pH value of the electrolyte. The surface potential can be expressed as [5,6,10]:

$$2.303(pH_{pzc} - pH) = \frac{q\Psi}{kT} + sinh^{-1}\left(\frac{q\Psi}{kT}\frac{1}{\beta}\right) \quad (1)$$

where pH_{pzc} is the pH value at the point of zero charge, k is Boltzmann's constant, T is the temperature of the system, and β is a parameter which reflects the chemical sensitivity of the gate insulator and is dependent on the density of surface hydroxyl groups. It is given by:

$$\beta = \frac{2q^2 N_S (K_b/K_a)^{1/2}}{kTC_{DL}} \tag{2}$$

where $N_S$is total number of surface sites per unit area, K_a and K_b are equilibrium constants of acid point and base point respectively, and C_{DL} is a simple capacitance derived by the Gouy-Chapman-Stern model. The site-binding model can be combined to the physics of the MOSFET (as model LEVEL 1 in SPICE [9]).

The result is an expression for the ISFET drain-source current (I_{DS}), where the modified threshold voltage (V_T) depends on pH value. For the saturation region:

$$I_{DS} = \frac{1}{2} K_n \left[(V_{GS} - V_T)^2 \right] \tag{3}$$

and for the linear region:

$$I_{DS} = K_n \left[(V_{GS} - V_T) - \frac{1}{2} V_{\mathrm{DS}} \right] \tag{4}$$

where K_n is the conduction parameter, V_{GS} the source gate voltage. V_T can be expressed as:

$$V_T = V_{TM} - \Phi_M/q + E_{Ref} + \chi^{Sol} - \Psi \tag{5}$$

where V_{TM} is the MOSFET's threshold voltage, $E_{ref}$is the potential of the reference electrode, $\chi^{Sol}$is the electrolyte-insulator surface dipole potential, $\Phi_M$is the work function of the metal gate (reference electrode) relative to vacuum [2].

In equation (5) all the parameters, with the exception of the surface potential, can be considered as a constant. So the threshold voltage depends only on the pH of the solution according to equation (1).

III. SIMULATION OF SURFACE POTENTIAL

The relationship between surface potential of a SnO_2 membrane and pH values was simulated from equations (1) and (2) and as is shown in Fig. 2.

The shape of the curves depend on N_S. The larger the N_S, the higher the pH sensitivity, and the more linear the response.

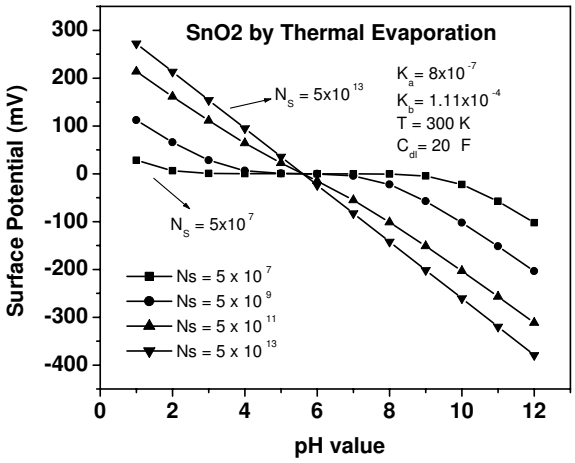

FIG. 2: Numerical simulation using site binding model of surface potential of tin oxide membrane versus pH value for different values of surface sites (N_S) using available parameters for thermally evaporated SnO_2 [10].

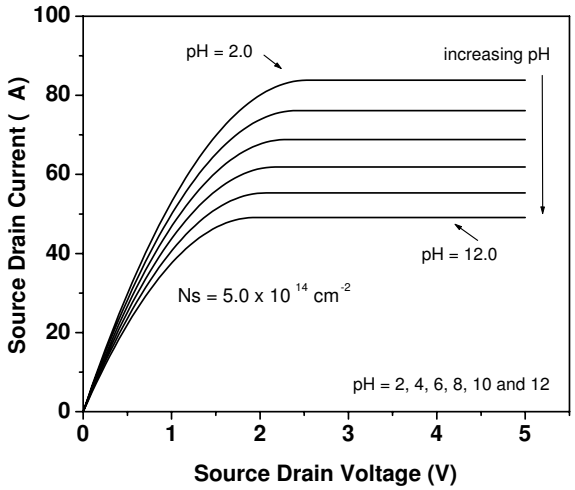

FIG. 3: Numerical simulation for ISFET. I_{DS} versus V_{DS} for varying pH values.

For a large N_S = 5 x 10^{14}cm^{-2}, the theoretical response of the device would be as presented in Fig. 3. Note that, for instance, variations of N_S could be associated to the structure of the SnO_2 film: increasing N_S values would be obtained from crystalline to amorphous material [11,12].

In summary, according to the numerical simulation, the optimized EGFET device should be fabricated using amorphous SnO_2. Nevertheless, up to date, most of the published works related to SnO_2 material properties deal with the crystalline phase only.

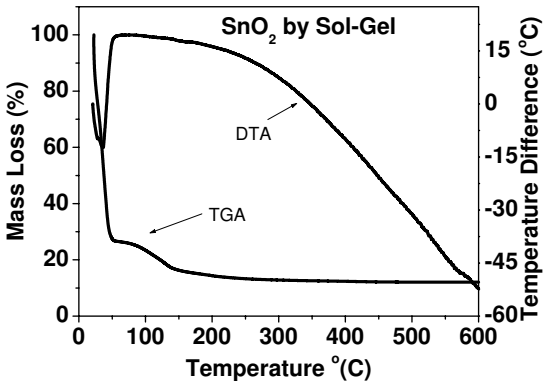

FIG. 4: TGA/DTA analysis for Sol-gel SnO_2.

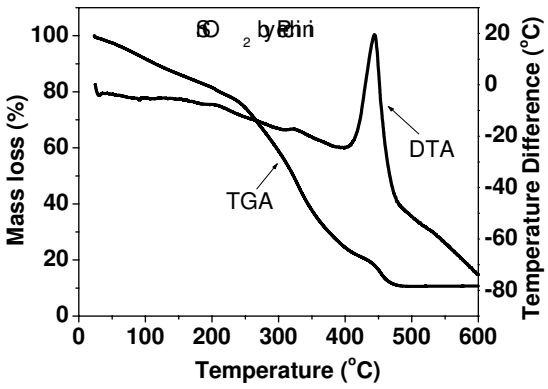

FIG. 5: TGA/DTA analysis for Pechini's SnO_2.

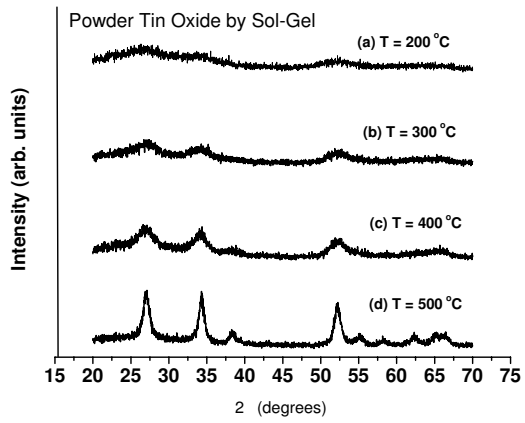

FIG. 6: XRD for sol-gel SnO_2 fabricated at (a) 200 (b) 300 (c) 400 and (d) 500^{o}C.

IV. EXPERIMENTAL PROCEDURE

In order to explore cheap and alternative SnO_2 EGFET fabrication processes, aluminum foils (1 mm-thick) were used as substrates. The SnO_2 was obtained by two methods: i) sol-gel [13] [8.37g of $SnCl_2H_2O$ are dissolved in 100 ml of absolute ethanol. This mixture is stirred and heated in reflux system at 80^{o}C for 2 hours] and ii) Pechini [14] [citric acid (60^{o}C) + Ethylene Glycol + Tin Citrate +HNO_3 (90^{o}C)]. Films were produced on the Al foils using brushing and calcination.

In order to accurately define the temperature at which the crystallization process begins and the purity of the material, the solution (TGA/DTA and FTIR) and final SnO_2 powder (FTIR and XRD) were investigated.

The electrical response of the sensor was measured using varying pH solutions and the curves were obtained by a HP4140B parameter analyzer.

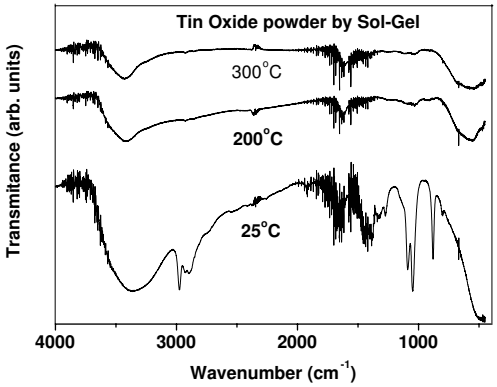

FIG. 7: FTIR for Sol-Gel SnO_2 solution (bottom curve) and calcinated at different temperatures.

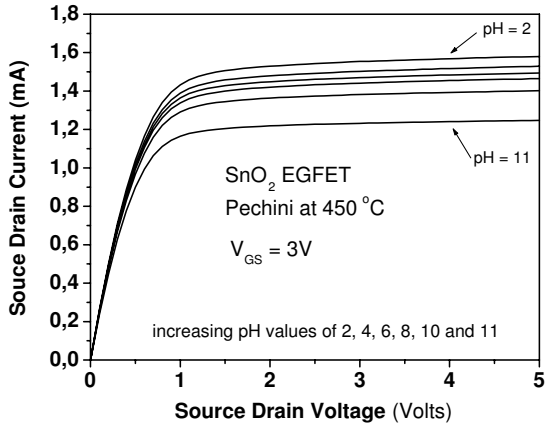

FIG. 8: Non-optimized response of a SnO_2 EGFET produced by Pechini at 450^{o}C.

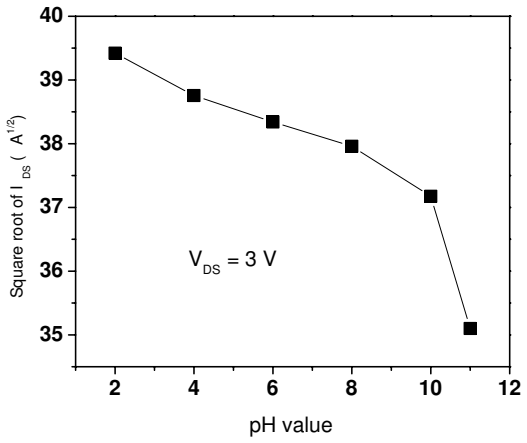

FIG. 9: Sensitivity of the pH sensor: linear response from pH=2 up to 10 in the saturation region.

V. RESULTS

The TGA/DTA results for the sol-gel SnO_2 solution are shown in Fig 4. Evaporation of several different species can be observed trough three slope changes on the curve. The weight loss above 100^0C may come from the condensation of remaining hydroxyl (SnOH) groups [13]. No appreciable weight change appears at temperatures exceeding 300^oC.

The TGA/DTA results for the Pechini's SnO_2 solution are shown in Fig. 5. An exothermic peak is observed above 400^oC, associated to the crystallization of the material. The organic compounds are removed from the SnO_2 sample above 300^oC for the sol-gel process and above 450^oC for the Pechini process. However, crystallization also occurs at 400^oC for Pechini's method. In this sense, pure and amorphous SnO_2 material cannot be obtained by this process.

XRD analysis were performed for both cases. The films produced by Pechini are crystalline above 400^oC (not shown here due to the lack of space). We present only the results for the sol-gel in Fig. 6. It can be observed that amorphous material can be obtained below 300^oC. Nevertheless, the material is not as pure as desired, as can be seen by the FTIR data shown in Fig. 7.

The SnO_2 absorption band is located close to 500 cm^{-1}, while the others correspond to water and organic compounds [15]. It can be observed that while the band at 1000cm^{-1} disappears at 200^oC, the other at 3500cm^{-1} remains noticeable even at 300^oC. This confirms the TGA/DTA suggestion that the amorphous material is not pure.

Fig. 8 shows the SnO_2 EGFET characterization for a non-optimized film produced by Pechini at a calcination temperature of 450^oC. The drain-current versus source-drain voltage is presented for varying pH concentrations from 2 up to 11. The sensitivity of the sensor in the saturation region, based on equation 3 is presented in Fig. 9. A linear response is observed from pH values 2 to 10.

VI. CONCLUSIONS

We used the sol-gel and Pechini's process to develop SnO_2 EGFET pH sensors. Both are cheaper and easier than common thin film techniques. The sol-gel fabricated devices did not succeed for processing temperatures below 300^oC, perhaps because of contamination by remaining organic compounds. The non-optimized Pechini's sensors, fabricated above 450^oC, have interesting linear response for pH values from 2 up to 10. The lowering of the processing temperature and the consequent fabrication of pure amorphous material would increase the number of surface sites, and lead to the final optimum device in the future.

Acknowledgements

This work was supported by FAPESP (01/08221-9, 03/08471-0), CAPES and CNPq, Brazil. We thank Prof. P. Olivi and Prof. J.M. Rosolen.

[1] M. Yunqing, C. Jianrong, and F. Keming, J. Biochen. Biophys. Methods (2005) in press.
[2] P. Bergveld, Sens. and Actuators B **88**, 1 (2003).
[3] L.-L. Chi, J.-C. Chou, W.-Y. Chung, T.-P. Sun, and S.-K Hsiung. Materials Chemistry and Physics **63**, 19 (2000).
[4] M.J. Schöning and A. Poghossian, The Analyst, **127**, 1137 (2002).
[5] J.-C. Chou and Y.-F. Wang. J. Appl Phys **41**, 5941 (2002).
[6] J.-C. Chou, P.-K., and Z-Jie Chen. J. Appl Phys **42**, 6790 (2003).
[7] D. E. Yates, S. Levine, and T.W. Healy. J. Chem. Soc. Fraday Trans. **1**, (1974).
[8] C. D. Fung, P. W. Cheung, and W.H. Ko, IEEE Trans. Electron Devices ED-33 **1**, 8 (1986).
[9] P. Antognetti and G. Massobrio, *Semiconductor Device Modeling with* SPICE (1988).
[10] H.-K Liao, Li-Lun Chi, J-C Chou, W-Y Chung, T-P Sun, and S-K H, Mat. Chem. and Phys. **59**, 6 (1999).
[11] D.-H Kwon, B.-W Cho, C.-S. Kim, and B.-K. Shon, Sens. and Actuators B **34**, 441 (1996).
[12] H.-K. Liao, J.-C. Chou, W.-Y. Chung, T.-P. Sun, and S.-K. Hsiung, Sens. and Actuators B **65**, 23 (2000).
[13] J. P. Chatelon, C. Terrier, and J.A Roger, Journal of Sol-Gel Science and Technology 10 (1997).
[14] E.C.P.E Rodrigues and P. Olivi, J. of Physics and Chemistry of Solids **64**, 1105 (2003).
[15] P. Siciliano, Sensors and Actuators B **70**, 153 (2000).